Volkov et al., http://www.jcb.org/cgi/content/full/jcb.201408083/DC1

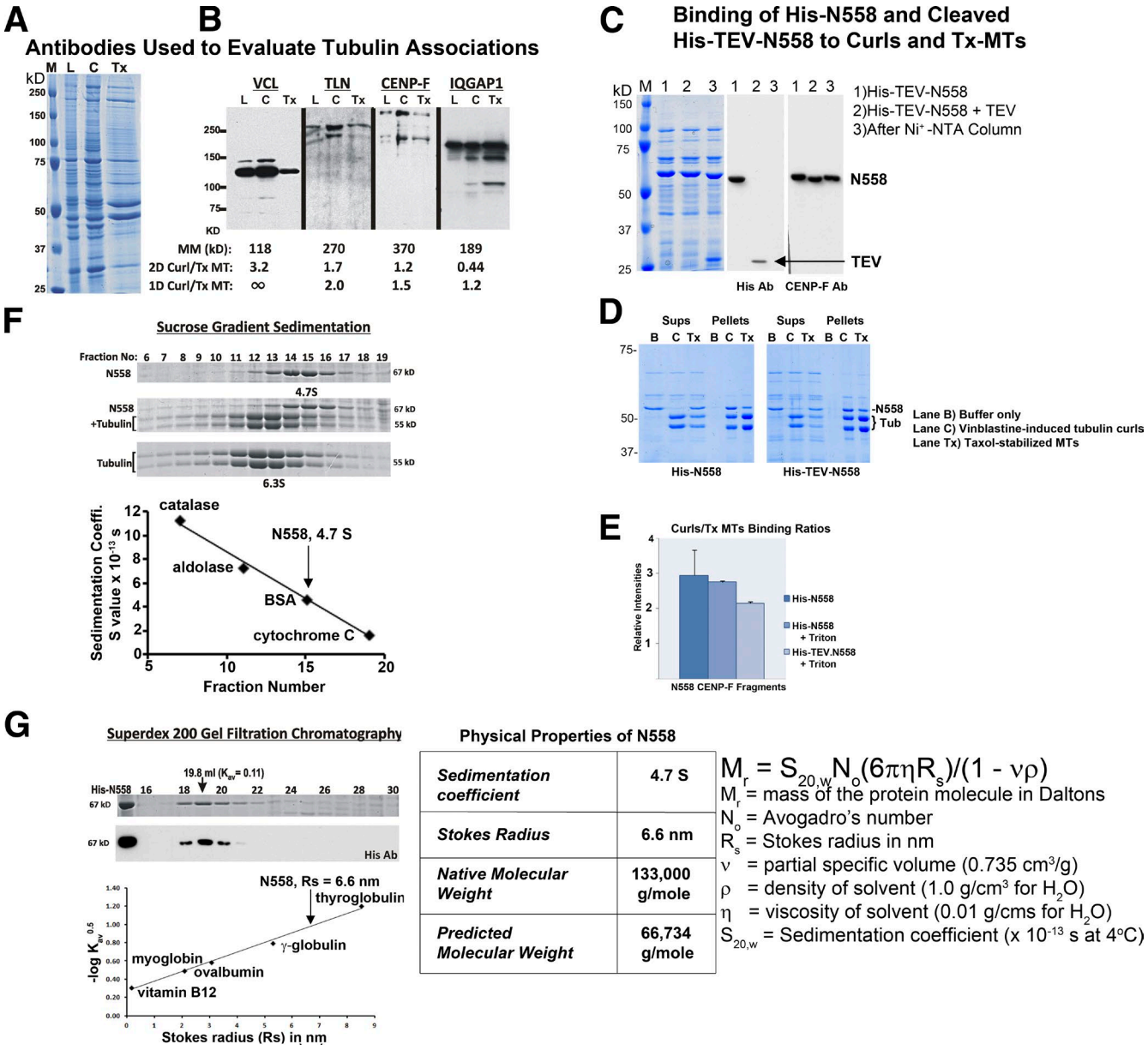

Figure S1. **Biochemical Studies.** (A and B) A test by immunoblotting of the relative binding to curls and Tx-MTs by four proteins of interests, based on mass spectrometry. U2OS cell extract (L) was mixed with either Vinblastine-induced tubulin curls (C) or Taxol-stabilized MTs (Tx) and pelleted. 4× the pellet volume of cell extract and equal volumes of each pellet were loaded onto 7% polyacrylamide gels (A), blotted to nitrocellulose paper, and then reacted with various primary antibodies to protein hits identified by mass spectrometry (B). Ratios of Curls/Tx-MTs counts from both mass spectrometry 1D and 2D runs are listed below each blot and in Tables S1 and S2. Antibodies to IQGAP were provided by N. Ahn. Antibodies to Vinculin (VCL) and Talin (TLN) were a gift of K. Burridge (University of North Carolina, Chapel Hill, NC). Antibodies to CENP-F were purchased from Santa Cruz Biotechnology, Inc. (C–E) A form of N558 that lacks the N-terminal 6-his tag shows a preference for curls over Tx-MTs that is almost as high as that seen with the tagged version. (C) Coomassie-stained SDS-PAGE of partially purified N558 with a TEV cleavage site between the CENP-F fragment and the 6-his tag, showing the removal of the tag by TEV protease. (D) Gels showing the relative amounts of α- and β-tubulin and N558 in the pull-downs by curls and Tx-MTs, as marked. (E) Ratios of N558 with and without the 6-his tag as pulled down by curls and Tx-MTs. Triton X-100 was added to the forms containing the TEV site to maintain sufficient solubility of the form with the 6-his tag removed. Error bars are SEMs from two to four experiments. (F) Fractions from a 5–20% sucrose gradient sedimentation of N558 and tubulin, together with sedimentation velocity standards. N558 sedimented at 4.7 S whether on its own or mixed with equimolar amounts of tubulin dimer in the presence of either GTP (as shown) or GDP (not depicted). (G) Elution behavior of N558 from a calibrated gel filtration column; the Stokes radius is 6.6 nm. The calculation of solution molecular mass was performed as in Siegel and Monty (1966).

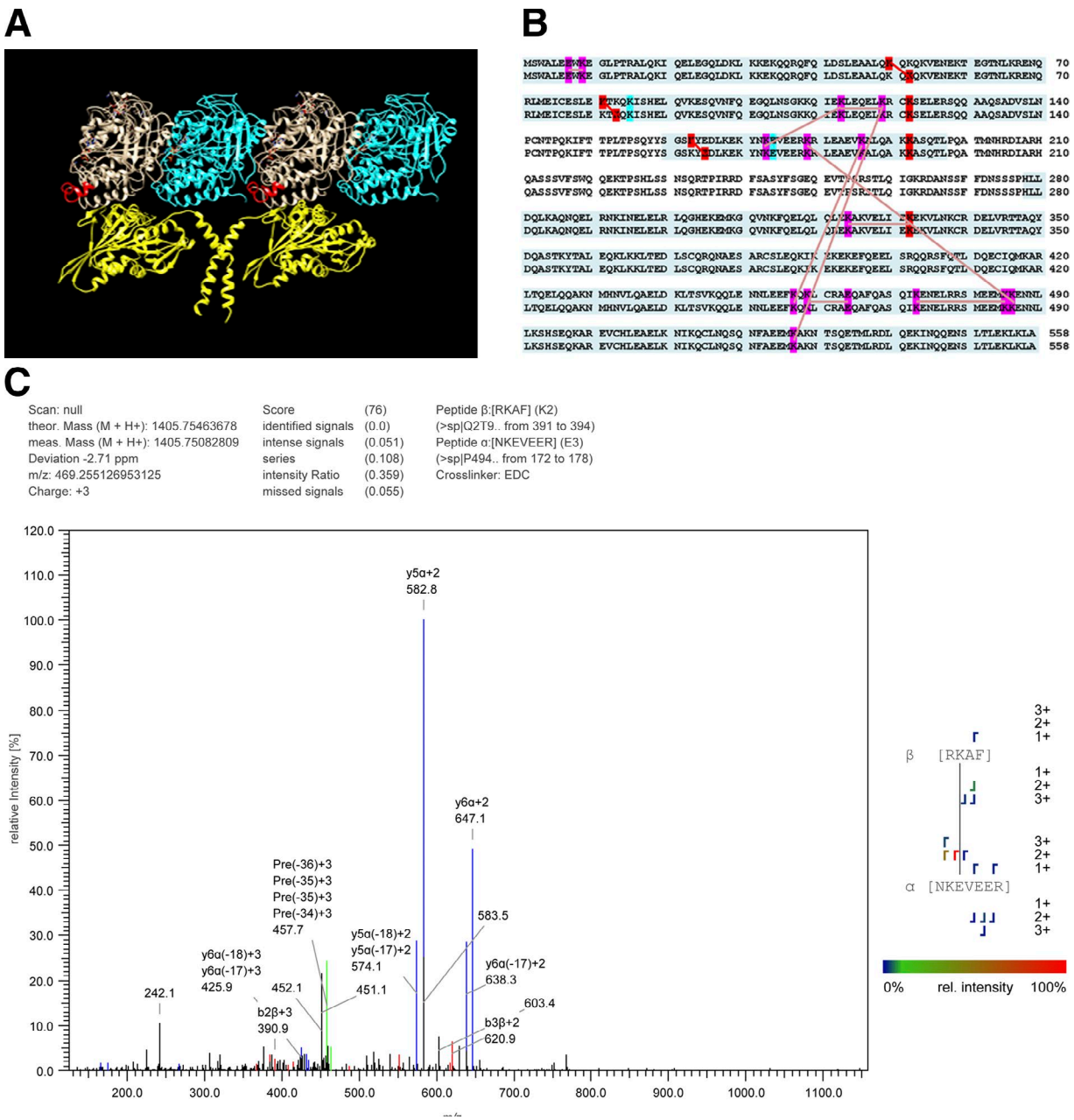

Figure S2. **Cross-linking by DSS of N558 to tubulin and to itself.** (A) An atomic model of two tubulin dimers (α-tubulin is cyan) bound to a dimer of kinesin (yellow) as a marker for the tubulin surface that faces out in a MT. Red marks the position of a peptide in β-tubulin that contains K392, which cross-linked twice with amino acids in N558. Image kindness of A. Hoenger (University of Colorado, Boulder, CO). (B) Primary structures of N558's two polypeptide chains in parallel with regions predicted to be coiled coils shaded in blue-gray. Cross-links made by both EDC and DSS are shown: red implies a link between chains; purple could be either between or within a chain; links between distant residues imply folds; and cyan marks residues linked to tubulin. (C) A spectrum from the mass spectrometric analysis of tryptic peptides obtained from N558 cross-linking with tubulin rings. This is from the EDC link between E174 of N558 to K392 of β-tubulin. All other cross-links shown in Fig. S2 B were similarly documented and are established with confidence.

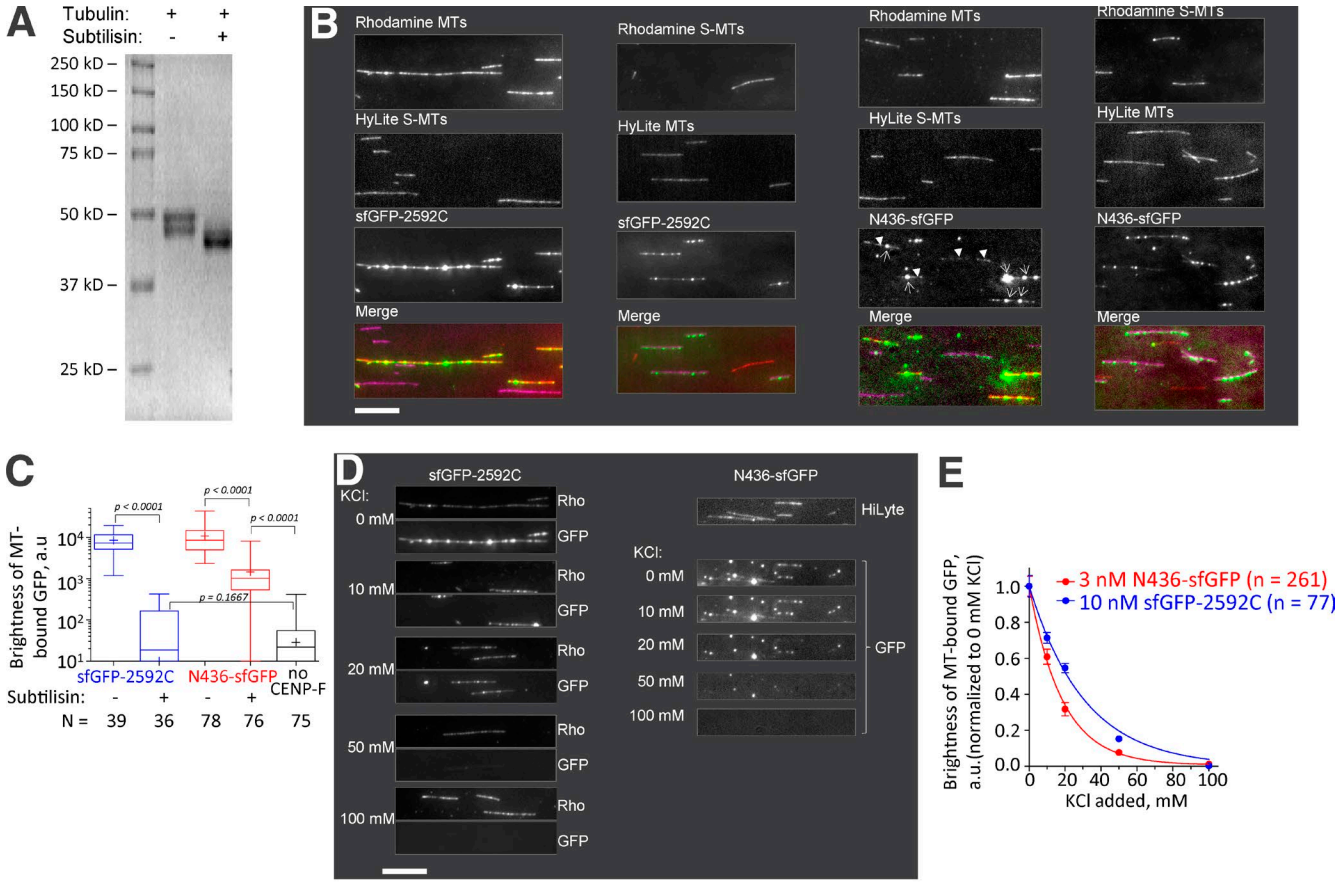

F

	N436-sfGFP	sfGFP-2592C
D, $\mu m^2/s$	0.163 ± 0.006	0.308 ± 0.006
K_{on}, $nM^{-1} \cdot s^{-1} \cdot 10^{-3}$	2.33 ± 0.19	0.548 ± 0.016
K_{off}, s^{-1}	2.27 ± 0.06	0.805 ± 0.012
K_D, µM	0.97 ± 0.08	1.47 ± 0.05
Residency time, s	0.427 ± 0.011	1.127 ± 0.015
Bleaching rate, s	12.2 ± 0.2	12.2 ± 0.2
Complex size, GFP molecules	2.6 ± 1.0	3.8 ± 0.2
Protein concentration in one chamber	5-50 pM	10 pM

Figure S3. **Effects of subtilisin, salt, and temperature on the binding of N436-sfGFP and sfGFP-2592C to the MTs**. (A) SDS-PAGE of Tx-MTs before and after treatment with subtilisin. (B) sfGFP-2592C (10 nM) binds to untreated MTs, but not to the subtilisin-treated MTs (S-MTs) in the same chamber. N436-sfGFP (3 nM) forms bright spots (arrows) and diffuse decoration (arrowheads) on untreated MTs, but only diffuse decoration on S-MTs. (C) MT-associated GFP fluorescence on regular and subtilisin-treated Tx-MTs in the presence of sfGFP-2592C (blue) or N436-sfGFP (red) or in the absence of CENP-F (black). P-values are reported for an unpaired *t* test. (D) Fluorescence of N436-sfGFP (3 nM) and sfGFP-2592C (10 nM) bound to Tx-MTs is reduced in the presence of KCl. (E) Quantification of mean intensity of MT-bound GFP as a function of KCl concentration. Bars, 10 µm. (F) Parameters of interaction of single molecules of N436-sfGFP and sfGFP-2592C with Tx-MTs.

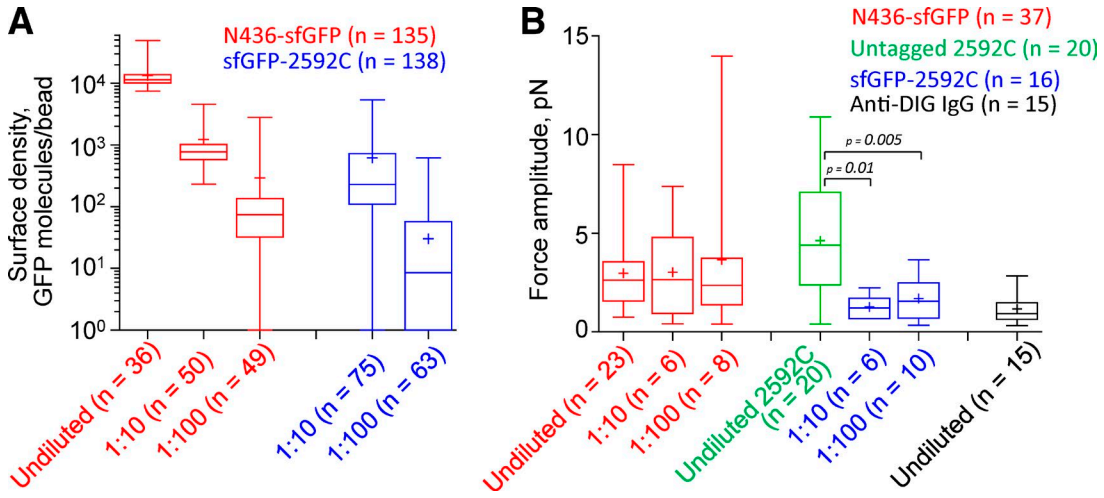

Figure S4. **MT-generated force as a function of reduced CENP-F density on the bead surface.** (A) Mean surface density of GFP on the beads coated with undiluted biotinylated anti-His tag IgG (Undiluted) and 1:10 and 1:100 molar mixtures of biotinylated anti-His tag IgG and biotinylated BSA. (B) MT-generated force measured using beads coated with various dilutions of CENP-F fragments or undiluted anti-DIG IgG. P-values are reported for an unpaired *t* test.

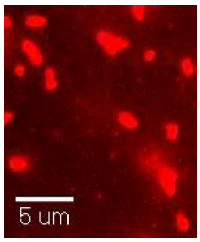

Video 1. **sfGFP-2592C tracks the depolymerizing MT end.** Time-lapse video of sfGFP-2592C (green) bound to a tethered, tripartite MT that was initially capped by rhodamine-labeled tubulin (red) assembled with GMPCPP and then uncapped by photobleaching, as described in Fig. 8. Both end tracking by an oligomer of the CENP-F fragment and diffusion of that fragment on the MT wall are visible. Images were acquired every 1 s for 192 s using an AxioImager Z1 microscope (Carl Zeiss).

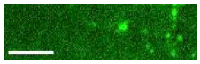

Video 2. **N436-sfGFP tracks the depolymerizing MT end.** Time-lapse video of N436-sfGFP (green) after the end of a segmented MT initially capped with rhodamine-labeled, GMPCPP-stabilized tubulin (red). Images were acquired every 0.5 s for 170 s using a custom-built TIRF setup based on an AxioImager Z1 microscope (Carl Zeiss).

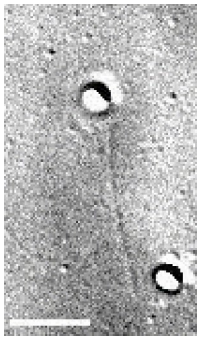

Video 3. **An N436-sfGFP–coated bead is transported by the MT end.** A bead coated with N436-sfGFP and allowed to bind to a tethered, tripartite MT. Photo-dissociation of the rhodamine-labeled cap (red) allows the MT to shorten, and the bead accompanies the moving MT tip, as described in Fig. 9. Images were acquired every 130 ms for 39 s using an AxioImager Z1 microscope (Carl Zeiss) using differential interference contrast optics.

Table S1 shows spectral counts for 2,879 proteins identified as binding to either Tx-MTs and/or curls of tubulin.

Table S2 shows spectral counts for selected cytoskeletal proteins binding to Tx-MTs and/or curls of tubulin, together with the computed binding ratios.

Reference

Siegel, L.M., and K.J. Monty. 1966. Determination of molecular weights and frictional ratios of proteins in impure systems by use of gel filtration and density gradient centrifugation. Application to crude preparations of sulfite and hydroxylamine reductases. *Biochim. Biophys. Acta.* 112:346–362. http://dx.doi.org/10.1016/0926-6585(66)90333-5